Dalton Transactions

ROYAL SOCIETY OF CHEMISTRY

COMMUNICATION

View Article Online
View Journal | View Issue

Check for updates

Cite this: *Dalton Trans.*, 2021, **50**, 14115

Received 7th July 2021,
Accepted 1st September 2021

DOI: 10.1039/d1dt02257a

rsc.li/dalton

Mn(I) phosphine-amino-phosphinites: a highly modular class of pincer complexes for enantioselective transfer hydrogenation of aryl-alkyl ketones†

Harikrishnan Jayaprakash

A series of Mn(I) catalysts with readily accessible and more π-accepting phosphine-amino-phosphinite (P′(O)N(H)P) pincer ligands have been explored for the asymmetric transfer hydrogenation of aryl-alkyl ketones which led to good to high enantioselectivities (up to 98%) compared to other reported Mn-based catalysts for such reactions. The easy tunability of the chiral backbone and the phosphine moieties makes P′(O)N(H)P an alternative ligand framework to the well-known PNP-type pincers.

The combination of chiral pincer ligands with base metals has been established to be effective in replacing precious noble metal catalysts in asymmetric reactions,[1–8] especially for hydrogenation of ketones.[9–17] Despite base metal catalysts being efficient, high synthetic costs and tedious synthetic protocols triggered the search for simpler and cheaper alternative chiral ligand frameworks with desired chirality.

Though the chiral base metal hydrogenation catalysts are known for decades, Mn(I) catalysts were left unexplored until 2016. Moreover, the Mn(I) complexes with classical chiral phosphines of the types PNP, PN(H)P, and PNN are commonly used for such reactions.[18–28] No efforts have been directed towards replacing phosphine pincers with electron-deficient[29] chiral bis-phosphinite (P(O)N(H)P(O)) or unsymmetrical phosphine-phosphinite pincer ligands (P′(O)N(H)P). Also, it must be noted that Mn(I) catalyzed asymmetric transfer hydrogenation (ATH) of ketones[18–23] is less explored compared to the asymmetric direct hydrogenation (AH).[24–28] Moreover, the observed enantioselectivities for ATH with well-defined Mn(I) catalysts **A**, **B** and **C** (Chart 1, 20%–85% ee) and further Mn(I) catalytic systems[21,23] (1%–90 ee%) are significantly lower when compared to those for AH (7%–99% ee).

The ligand precursors **1a** and **1b** were prepared by the condensation of the corresponding aldehydes **5a** and **5b** with relatively cheap and readily available (1*S*,2*S*)-2-aminocyclohexan-1-ol in methanol at room temperature, followed by their *in situ* reduction with sodium tetrahydridoborate. Deprotonation of **1a** and **1b**, followed by the addition of PR'_2Cl, resulted in the formation of ligands **2a** and **2b** with 95–96% purity as determined by $^{31}P\{^1H\}$ NMR.[19,29] The desired $[Mn(CO)_2(\mathbf{2a–2b})]Br$ (**3a** and **3b**) were then obtained as a yellow solid upon reacting **2a** and **2b** with $[MnBr(CO)_5]$ in toluene (Scheme 1, see the ESI†).

The $^{31}P\{^1H\}$ NMR spectra of **3a** and **3b** exhibit an AX system that suggests mutually *trans* positioned nuclei.[19,29] The IR spectra of complexes **3a** (1931 cm^{-1}, 1851 cm^{-1}, Fig. 2) and **3b** (1930 cm^{-1}, 1850 cm^{-1}) show two strong CO bands of similar intensity which further support the presence of mutually *cis*-oriented CO ligands which are in agreement with the previously reported Mn(I) carbonyl pincer complexes.[19,29] The spectroscopic evidence taken together points to the formation of *cis*, *mer*-$[MnBr(CO)_2(\mathbf{2a–2c})]$ (**3a** and **3b**). In fact, such a structure was also confirmed by X-ray crystallography in the case of **3a** (Fig. 1, see the ESI† for more details).

Notably, the **Mn1–P2** bond length of **Mn1** with phosphorus atom **P2** (2.227 Å) is shorter than that for **Mn1–P1** (2.308 Å). Moreover, a comparison of the IR stretching frequency of **3a** with that of its homologous *trans* bis-phosphine pincer complex **11** (1921 cm^{-1}, 1842 cm^{-1}, Fig. 2; see the ESI† for the synthesis) suggests that phosphinite (**P2**) is a weaker electron donor and possesses better dπ–pπ back bonding (M → L back

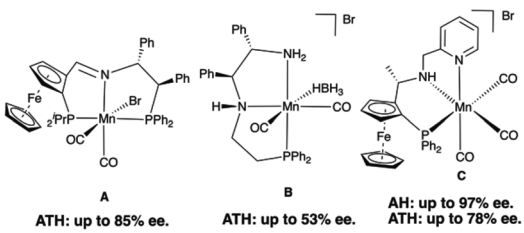

Chart 1 Examples of chiral Mn(I) catalysts for the asymmetric transfer (ATH) and direct hydrogenation (AH) of ketones.

Department of Chemistry and Applied Biosciences, ETH Zürich, Wolfgang-Pauli-Str. 10, CH-8093 Zürich, Switzerland. E-mail: hari@inorg.chem.ethz.ch

† Electronic supplementary information (ESI) available. CCDC 2083796. For ESI and crystallographic data in CIF or other electronic format see DOI: 10.1039/d1dt02257a

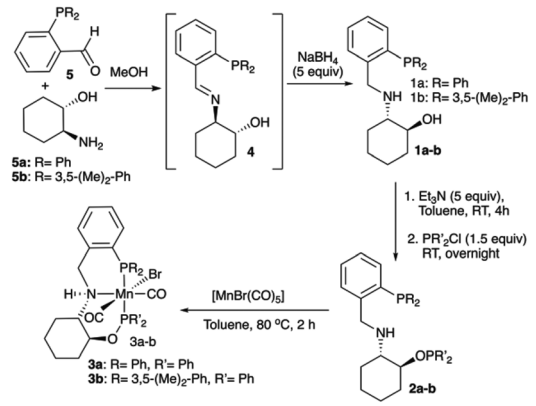

Scheme 1 Synthesis of the ligands (**2a** and **2b**) and complexes (**3a** and **3b**).

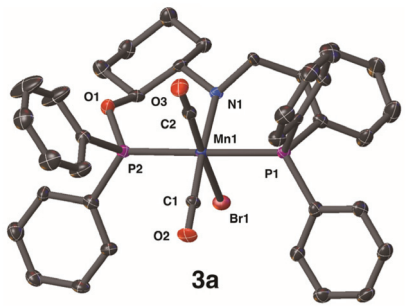

Fig. 1 ORTEP plot of **3a** (ellipsoid sets at 40% probability). Selected bond lengths [Å] and angles [°]: P(1)–Mn(1) 2.3083(19), P(2)–Mn(1) 2.2274(19), C(1)–Mn(1) 1.758(8), C(2)–Mn(1) 1.779(7), P(2)–Mn(1)–C(2) 88.7(2) and P(2)–Mn(1)–Br(1) 89.74(6).

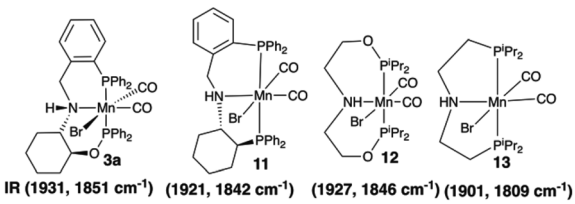

Fig. 2 Comparison of the IR stretching frequency of Mn(I) phosphine and phosphinite pincer complexes.

donation) compared to phosphine **P1**. The observed CO stretching frequencies are analogous to those of the previously reported Mn(I) bis-phosphine (**12**) and bis-phophinite complex (**13**).[29,30]

The activity of **3a** was next investigated in ATH with 2-acetonaphthone (**8a**) as a prototypical substrate[31] under a broad range of conditions. The reaction temperature and nature of the base and catalyst have the largest effect on the enantioselectivity and activity of the catalytic system. A strong base is necessary to achieve high activity of catalyst **3a** and notably, catalyst **3b** (82% ee) has shown better enantioselectivity in comparison with **3a** (79% ee, see the ESI†). The activity of the complex **3a** was found to be diminishing with increasing temperature from 40 °C to 80 °C (see the ESI†). It is noteworthy that the tendency of Mn(I) complexes to form a metal-aziridine intermediate at high temperature and an amido species at lower temperature has been previously reported.[32] Therefore, it is expected that **4a** and **4b** are formed at 40 °C and 80 °C, respectively, leading to different reactivities at the corresponding temperatures (see Scheme 4 for the proposed mechanism). The greater acidity of the benzylic proton and better dπ–pπ back bonding of the phosphinite ligand possibly lead to the easier formation of metal-aziridine intermediate **4b** that remains as the resting species. This could prevent the formation of **5a** which could be a possible explanation for the lower activity of **3a** at higher temperatures (Scheme 2). A poisoning test with trimethyl phosphine (30 mol% *vs.* **3a**) and the fact that the enantioselectivity remains the same throughout the reaction indicate the presence of a homogeneous catalytic system.[33,34]

Hence, with the identified optimal reaction conditions **C1** (catalytic loading (**3b**) 2 mol%, 4 mol% *t*BuOK (1 M in THF), 40 °C, 18 h, 0.2 M, Scheme 2), the ATH of a large scope of aryl-

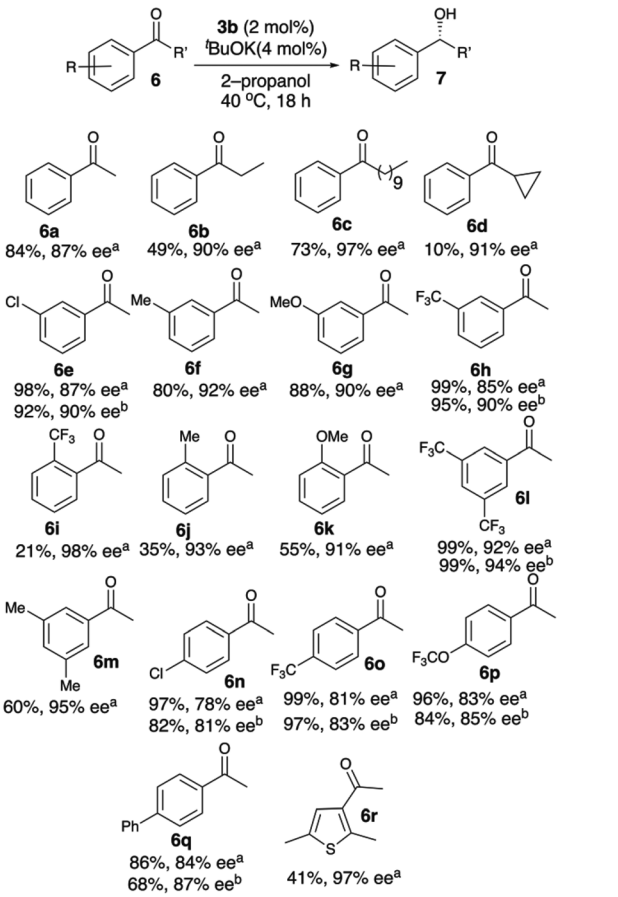

Scheme 2 Asymmetric transfer hydrogenation with catalyst **3b**: isolated yields are given and ee values were determined by GC and HPLC, respectively. [a] Optimized conditions **C1** (catalytic loading: 2 mol%, 4 mol% *t*BuOK, 40 °C, 18 h, 0.2 M). [b] Re-optimized conditions **C2** (catalytic loading: 1 mol%, 2 mol% *t*BuOK, RT, 24 h).

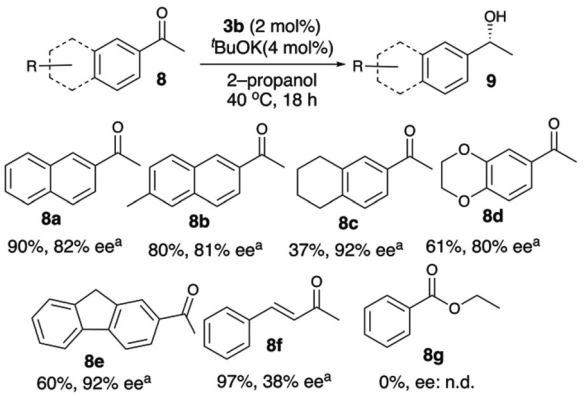

Scheme 3 Asymmetric transfer hydrogenation with catalyst **3b**. Reaction conditions **C1** (catalytic loading: 2 mol%, 4 mol% *t*BuOK, 40 °C, 18 h, 0.2 M). [a]Isolated yields are given and ee values were determined by GC and HPLC, respectively.

alkyl ketones was investigated (see Schemes 2 and 3). The corresponding secondary alcohols were obtained in good yields with high enantioselectivities (80%–98% ee). With acetophenones, **3b** tolerates *ortho*, *meta* and *para* substituents, with enantioselectivities in the order of *ortho* (91%–98% ee) > *meta* (90%–92% ee) > *para* (82%–87% ee) substituents and yields in the order of *meta*, *para* (68%–99%) > *ortho* (21%–55%) substituents.

Meta-substituted acetophenones (**6e–6g**) including 3,5 disubstituted acetophenone (**6m**) give high enantioselectivities (up to 94% ee, Scheme 2) and quantitative yields. Catalyst **3b** gives the trifluoromethyl-substituted alcohols **7h** and **7l** which are important synthons for fungicides[35] and NK_1 antagonists[35] in quantitative yields and with 90% and 94% ee, respectively. It is to be noted that these are the best enantioselectivities observed with *meta*-chloro-acetophenone (**6e**, 90% ee) and 3,5-bis-trifluoromethyl-acetophenone (**6l**, 94% ee) for reported manganese complexes for ATH (24–85% ee, 6–85% ee, respectively).[18,19,21–23]

Challenging substrates like *ortho*-substituted acetophenones (**6i–6k**) displayed high enantioselectivity (91–98% ee), though with lower yield, likely due to the greater steric hindrance of the system (Scheme 2). Despite such shortcomings, the observed enantioselectivities are the highest for *ortho*-methoxyacetophenone (**6k**, 91% ee) in comparison with other reported manganese catalysts for ATH (61–90% ee).[18,19,21–23]

Para-substituted acetophenones (**6o–6p**) were reduced by **3b** with quantitative yields, albeit with significantly lower enantioselectivities (82–87%). The use of lower temperature, *i.e.*, room temperature and a catalytic loading of 1 mol% (re-optimized conditions **C2**: catalytic loading 1 mol%, 2 mol% *t*BuOK, RT, 24 h) allows the improvement of enantioselectivity while maintaining good yields. The highest difference in enantioselectivity was observed with the electron-rich *para*-substituted acetophenone (**6q**, by 4%). Moreover, these conditions improved the observed enantioselectivities for electron-deficient *meta* acetophenones (**6e** and **6h** by 3% and 4%, respectively) or 3,5 disubstituted acetophenone (**6l** by 2%). It is again noteworthy that catalyst **3b** provides high enantiomeric excess (83% ee) with *para*-trifluoromethyl-acetophenone (**6o**) when comparing with other Mn-based catalysts for ATH (55–76% ee).[18,19,21–23] The heterocycle **6r** was also reduced by **3b** with high enantioselectivity (97% ee) but with lower yield (25% and 41%, respectively).

Alkyl-phenyl ketones with various alkyl substituents were also investigated for their reactivity with catalyst **3b**. Ethyl phenyl ketone (**6b**) has shown a higher ee (90%) and a lower isolated yield (49%) compared to acetophenone (**6a**, 86% ee and 84% yield) and the trend remains the same with further increase in the alkyl chain length (**6c**, Scheme 2). Since these catalysts are highly sensitive towards steric hindrance, their activity with 2° alkyl-aryl ketone **6d** (91% ee and 10% yield) is greater than that with 3° alkyl-aryl ketones. Substrates with high steric bulk such as cyclohexyl phenyl ketone, 2-methoxybenzophenone and tertiary butyl phenyl ketone do not get reduced with the catalyst **3b**.

The extended aromatic ketones **8a** and **8b** were reduced with 82% ee (Scheme 3). Both 2-acetyl-fluorene (**8e**) and tetralone (**8c**) showed a higher ee of 92% when compared with **8a**; however, **8d** gave a lower ee of 80%. It is noteworthy that α,β-unsaturated ketones (**8f**) have shown low enantioselectivity (38% ee) since the carbonyl group is placed remotely from the aryl ring. The enantioselectivity observed with **8a** (82% ee) is

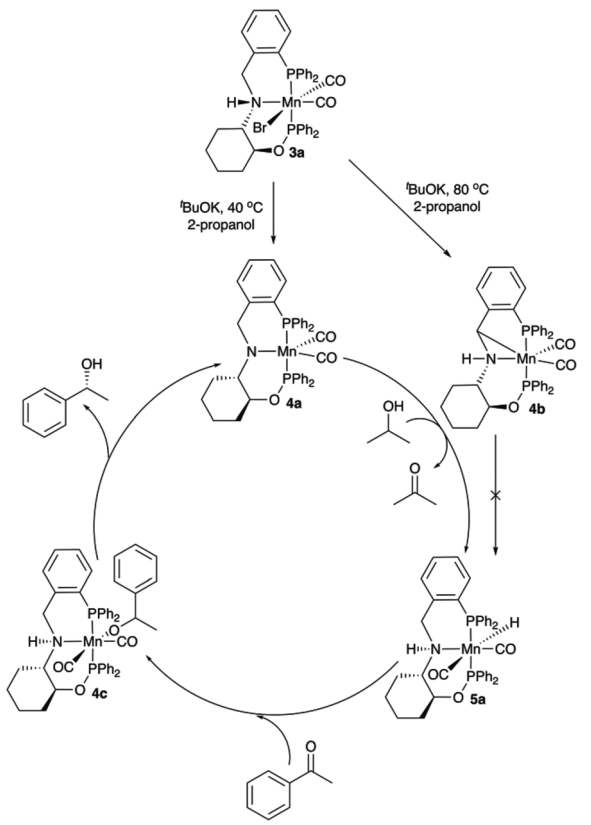

Scheme 4 Proposed mechanism for asymmetric transfer hydrogenation of acetophenone with **3a**.

the highest on comparing with other Mn(I) catalysts (up to 76% ee) for ATH.[18,19,21–23] The "*R*" isomer is formed as the major enantiomer during the reduction of ketones with **3b**. The aromatic ester **8g** was also not reduced with complex **3b** (Scheme 3).

Based on the experimental results obtained by the screening of the catalysts **3a** and **3b** and the reported Mn(I) intermediates,[32] a possible reaction mechanism in which temperature is the key parameter is proposed (Scheme 4). As discussed earlier, the higher activity of the catalyst at 40 °C could be due to the possible formation of the Mn(I) amido species **4a**. The Mn(I) amido species **4a** formed at 40 °C in the presence of *t*BuOK leads to the possible formation of hydride **5a** *via* oxidation of 2-propanol. An *Re* or *Si* selective hydride attack on acetophenone leads to the formation of **4c**. The intermediate **4c** then regenerates **4a** by eliminating the enantioenriched alcohol.

In conclusion, readily accessible chiral pincer ligands (**2a** and **2b**) and their corresponding well-defined Mn(I) complexes (**3a** and **3b**) were developed. The complex **3b** shows high enantioselectivities (80%–97% ee) for the ATH of ketones, thus outperforming other Mn(I) catalysts. This demonstrates that the ligand scaffolds like **2** are a valuable alternative to the conventional chiral phosphine pincers (PN(H)P) as they are cheap and highly modular. Most importantly this class of ligands can be even extrapolated to various other asymmetric catalytic applications. Further studies on the catalytic system will be carried out in the future.

Conflicts of interest

There are no conflicts to declare.

Acknowledgements

I thank the Swiss National Science Foundation for financial support (grant no. 200020_184606) and Prof. Antonio Mezzetti for his contribution in the initial phase of the project. I also thank Dr Jordan Meyet and Dr Michael. D. Wörle for the single-crystal X-ray analysis. I sincerely thank Profs. Antonio Togni, Christophe Copéret and Hansjörg Grützmacher for their most valuable assistance in finalizing the manuscript and for their general support.

References

1 S. Murugesan and K. Kirchner, *Dalton Trans.*, 2016, **45**, 416–439.
2 D. Benito-Garagorri and K. Kirchner, *Acc. Chem. Res.*, 2008, **41**, 201–213.
3 S. K. Gibbons, Z. Xu, R. P. Hughes, D. S. Glueck and A. L. Rheingold, *Organometallics*, 2018, **37**, 2159–2166.
4 H. Valdés, M. A. García-Eleno, D. Canseco-Gonzalez and D. Morales-Morales, *ChemCatChem*, 2018, **10**, 3136–3172.
5 K. Junge, V. Papa and M. Beller, *Chem. – Eur. J.*, 2019, **25**, 122–143.
6 G. Bauer and X. Hu, *Inorg. Chem. Front.*, 2016, **3**, 741–765.
7 Y. Xiang, Q. Ge, S. Wu, X. Zheng and Z. Yang, *RSC Adv.*, 2020, **10**, 9563–9578.
8 A. Casnati, M. Lanzi and G. Cera, *Molecules*, 2020, **25**, 3889.
9 M. Garbe, Z. Wei, B. Tannert, A. Spannenberg, H. Jiao, S. Bachmann, M. Scalone, K. Junge and M. Beller, *Adv. Synth. Catal.*, 2019, **361**, 1913–1920.
10 (*a*) F. Agbossou-Niedercorn and C. Michon, *Coord. Chem. Rev.*, 2020, **425**, 213523; (*b*) J. Wen, F. Wang and X. Zhang, *Chem. Soc. Rev.*, 2021, **50**, 3211–3237; (*c*) Y. Wang, M. Wang, Y. Li and Q. Liu, *Chem*, 2021, **7**, 1180–1223.
11 A. Passera and A. Mezzetti, *Adv. Synth. Catal.*, 2019, **361**, 4691–4706.
12 J. F. Sonnenberg, A. J. Lough and R. H. Morris, *Organometallics*, 2014, **33**, 6452–6465.
13 A. Zirakzadeh, K. Kirchner, A. Roller, B. Stöger, M. Widhalm and R. H. Morris, *Organometallics*, 2016, **35**, 3781–3787.
14 S. A. M. Smith, P. O. Lagaditis, A. Lüpke, A. J. Lough and R. H. Morris, *Chem. – Eur. J.*, 2017, **23**, 7212–7216.
15 R. Huber, A. Passera and A. Mezzetti, *Organometallics*, 2018, **37**, 396–405.
16 P. O. Lagaditis, P. E. Sues, J. F. Sonnenberg, K. Y. Wan, A. J. Lough and R. H. Morris, *J. Am. Chem. Soc.*, 2014, **136**, 1367–1380.
17 R. Huber, A. Passera and A. Mezzetti, *Chem. Commun.*, 2019, **55**, 9251–9266.
18 A. Zirakzadeh, S. R. M. M. de Aguiar, B. Stöger, M. Widhalm and K. Kirchner, *ChemCatChem*, 2017, **9**, 1744–1748.
19 K. Z. Demmans, M. E. Olson and R. H. Morris, *Organometallics*, 2018, **37**, 4608–4618.
20 C. S. G. Seo, B. T. H. Tsui, M. V. Gradiski, S. A. M. Smith and R. H. Morris, *Catal. Sci. Technol.*, 2021, 3153–3163.
21 K. Azouzi, A. Bruneau-Voisine, L. Vendier, J. B. Sortais and S. Bastin, *Catal. Commun.*, 2020, **142**, 106040.
22 R. Van Putten, G. A. Filonenko, A. Gonzalez De Castro, C. Liu, M. Weber, C. Müller, L. Lefort and E. Pidko, *Organometallics*, 2019, **38**, 3187–3196.
23 J. Schneekönig, K. Junge and M. Beller, *Synlett*, 2019, 503–507.
24 M. B. Widegren, G. J. Harkness, A. M. Z. Slawin, D. B. Cordes and M. L. Clarke, *Angew. Chem., Int. Ed.*, 2017, **56**, 5825–5828.
25 M. B. Widegren and M. L. Clarke, *Catal. Sci. Technol.*, 2019, **9**, 6047–6058.
26 L. Zhang, Y. Tang, Z. Han and K. Ding, *Angew. Chem., Int. Ed.*, 2019, **58**, 4973–4977.
27 (*a*) M. Garbe, K. Junge, S. Walker, Z. Wei, H. Jiao, A. Spannenberg, S. Bachmann, M. Scalone and M. Beller, *Angew. Chem., Int. Ed.*, 2017, **56**, 11237–11241; (*b*) F. Ling, H. Hou, J. Chen, S. Nian, X. Yi, Z. Wang, Di. Song and W. Zhong, *Org. Lett.*, 2019, **21**, 3937–3941.

28 L. Zeng, H. Yang, M. Zhao, J. Wen, J. H. R. Tucker and X. Zhang, *ACS Catal.*, 2020, **10**, 13794–13799.
29 H. Li, D. Wei, A. Bruneau-Voisine, M. Ducamp, M. Henrion, T. Roisnel, V. Dorcet, C. Darcel, J. F. Carpentier, J. F. Soulé and J. B. Sortais, *Organometallics*, 2018, **37**, 1271–1279.
30 S. Fu, Z. Shao, Y. Wang and Q. Liu, *J. Am. Chem. Soc.*, 2017, **139**, 11941–11948.
31 According to the preliminary DFT studies, the π–π interaction between the aryl rings on the ligand phosphine atom (not the aryl rings on the phosphinite donor) and the incoming ketones plays the key role in the enantioselectivity of our reaction. Hence 2-acetonaphthone was chosen as the prototypical substrate over acetophenone (unpublished results).
32 S. Chakraborty, U. Gellrich, Y. Diskin-Posner, G. Leitus, L. Avram and D. Milstein, *Angew. Chem., Int. Ed.*, 2017, **56**, 4229–4233.
33 R. H. Crabtree, *Chem. Rev.*, 2012, **112**, 1536–1554.
34 Y. Li, S. Yu, X. Wu, J. Xiao, W. Shen, Z. Dong and J. Gao, *J. Am. Chem. Soc.*, 2014, **136**, 4031–4039.
35 (*a*) K. Tanaka, M. Katsurada, F. Ohno, Y. Shiga, M. Oda, M. Miyagi, J. Takehara and K. Okano, *J. Org. Chem.*, 2000, **65**, 432–437; (*b*) K. M. J. Brands, J. F. Payack, J. D. Rosen, T. D. Nelson, A. Candelario, M. A. Huffman, M. M. Zhao, J. Li, B. Craig, Z. J. Song, D. M. Tschaen, K. Hansen, P. N. Devine, P. J. Pye, K. Rossen, P. G. Dormer, R. A. Reamer, C. J. Welch, D. J. Mathre, N. N. Tsou, J. M. McNamara and P. J. Reider, *J. Am. Chem. Soc.*, 2003, **125**, 2129–2135.